Experimental Study on Forced Convection Heat Transfer of Helium Gas through a Minichannel

Xu, Feng

Liu, Qiusheng

Shibahara, Makoto

(Citation)
International Journal of Heat and Mass Transfer,171:121117

(Issue Date)
2021-06

(Resource Type)
journal article

(Version)
Accepted Manuscript

Experimental Study on Forced Convection Heat Transfer of Helium Gas through a Minichannel

Feng Xu, Qiusheng Liu*, Makoto Shibahara
Department of Marine Engineering, Graduate School of Maritime Sciences, Kobe University, 5-1-1, Fukaeminami-machi, Higashinada-ku, Kobe 658-0022, Japan
(* Corresponding author. E-mail: qsliu@maritime.kobe-u.ac.jp)

Abstract

For the development of thermal efficiency and security of fusion reactors, it is vital to know the heat transfer process for helium gas cooling in the fusion blanket. In this paper, an experimental study was performed on the heat transfer characteristics for turbulent flow in a horizontal minichannel employing helium gas as the working fluid. A circular platinum tube with an inner diameter of 1.8 mm was heated by direct current and cooled by helium gas. The heat input was exponentially increased with a relatively long e-folding time of the heat generation rate. The obtained experimental data were compared with the predictions on classical correlations applied to conventional channels. The influence of various experimental parameters on the heat transfer coefficient was clarified. Based on the results, heat transfer enhancement was confirmed in the minichannel compared with the conventional channel. The heat transfer coefficient increased with increasing flow velocity and decreased as the ratio of inner surface temperature to gas bulk temperature increased. An empirical correlation for turbulent flow of helium gas in a minichannel with a deviation of ±10% was derived from a large quantity of experimental data.

Keywords: Heat transfer enhancement; Helium gas; Forced convection; Minichannel; e-folding time; Empirical correlation

Nomenclature

A	inner surface area of test heater, m^2
a	thermal diffusivity, m^2/s
c_h	specific heat of test heater, J/(kg·K)

c_p specific heat at constant pressure, J/(kg·K)

d inner diameter of test heater, m

f friction factor

h heat transfer coefficient, W/(m^2·K)

I direct current, A

L_e effective length of test heater, m

Nu Nusselt number

n slope

P pressure, kPa

Pr Prandtl number

Q heat generation rate, W

Q_0 initial exponential heat generation rate per unit volume, W/m^3

$\dot{Q}$ heat generation rate per unit volume, W/m^3

q heat flux, W/m^2

Re Reynolds number

R_s standard resistance, Ω

R_T resistance of test heater, Ω

r radius of test heater, m

T temperature, K

T_a average temperature of test heater, ºC

T_s inner surface temperature of test heater, ºC

ΔT temperature difference between inner surface temperature of test heater and average gas bulk temperature, K

t time, s

u flow velocity, m/s

V volume of test heater, m^3

V_I voltage drop across standard resistor, V

V_R voltage drop across test heater, V

V_T unbalanced voltage difference, V

Greek symbols

λ thermal conductivity, W/(m·K)

μ dynamic viscosity, Pa·s

ν	kinematic viscosity, m^2/s
ρ	density, kg/m^3
τ	e-folding time of heat generation rate, s

Subscripts

f	fluid
g	gas
h	heater
i	inner
in	inlet of test heater
ipt	inlet pressure transducer
o	outer
opt	outlet pressure transducer
out	outlet of test heater
w	wall of test heater

1. Introduction

Helium gas is a promising coolant candidate for fusion reactor because of its high-temperature capability, chemical inertness, and neutron transparency [1]. The application of helium gas in the blanket of fusion reactor was reported by Boccaccini et al. [2] and Xiang et al. [3]. The plasma-facing first wall is designed to withstand an enormous amount of heat load in the fusion reactor. The heat load will increase rapidly in a short time as plasma disruption occurs. The heat is removed by the high-pressure helium gas passing through many channels configured in the blanket [4]. To enhance the heat transfer performance, downsizing of channels is an available method such as a microchannel and minichannel. This technology is initially developed for integrated circuits but can also be applied in miniature heat exchange elements [5]. In terms of channel categories presented by Kandlikar [6], flow channels with hydraulic diameters ranging from 200 μm to 3 mm are defined as minichannels, which are different from conventional channels. Therefore, it is crucial to clarify the heat transfer performance for helium gas flowing inside the minichannel.

Concerning research on the heat transfer process in minichannels, many researchers have focused on single-phase liquid flow, especially water. Nakamura et al.

[7] employed water as the working fluid and utilized circular tubes with inner diameters of 0.7, 1.0, and 3.0 mm as test heaters. The heat transfer coefficients were enhanced as the inner diameters of the tubes were reduced. The obtained experimental heat flux was higher than the predicted value of some classic correlations used for conventional channels under the same conditions. Nguyen et al. [8] studied the laminar and turbulent flow of water inside a trapezoidal shape minichannel experimentally and numerically. The results showed that the critical Reynolds number is 1285, which is earlier than the traditional transition zone of laminar to turbulent. Adams et al. [9] confirmed that the heat transfer performance for water flowing inside circular ducts with 0.76 and 1.09 mm as diameters is intensified compared to conventional large-diameter channels. The correlation proposed by Gnielinski [10] was modified considering the effect of inner diameter. Moreover, concerning other liquids, Dai et al. [11] studied the thermal-hydraulic characteristics of ethanol flowing inside rectangular and circular channels with hydraulic diameters of 0.715 and 0.86 mm, respectively. They concluded that the scaling effects play a crucial role in the thermal characteristics of minichannels. Li et al. [12] conducted experiments on turbulent flow in circular minichannels with FC-72 serving as the working fluid. A new empirical correlation of minichannel was derived from their experimental data, which agrees well with the correlation presented by Adams et al. [9]. Li et al. [13] also studied the transient heat transfer for FC-72 flowing in minichannels. A Fourier number was introduced to describe the effect of the exponential period (e-folding time). Owhaib and Palm [14] experimentally researched the heat transfer performance of single-phase forced convection of R134a in small diameter circular tubes. The experimentally obtained data agreed well with the classical correlations in the turbulent region.

However, there are few studies conducted on the turbulent heat transfer performance of helium gas passing through the minichannel. Mylavarapu et al. [15] carried out thermal-hydraulic experiments on helium gas flowing in a semi-circular channel with a 1.22 mm hydraulic diameter in printed circuit heat exchangers. Although the relationship between the Nusselt numbers and Reynolds numbers behaved a similar trend with the conventional circular tube correlation, the Nusselt numbers obtained by experimental data were relatively larger than those from the circular pipe correlation in the laminar region. Jiao et al. [16] focused on the effect of thermophysical properties of helium gas with a large temperature variation. They found that the local Nusselt number increases with a decrease in the local Reynolds number along the flow direction due to

the significant difference in the gas temperature. Arbeiter [17] used an annular duct with a hydraulic diameter of 1.2 mm and a rectangular channel with a hydraulic diameter of 1.96 mm to investigate the thermal-hydraulic performance of such cooling gas as helium, argon, air, and nitrogen. The experimental results showed good overall agreement with the classic correlations. Our previous work [18] focused on the transient heat transfer for helium gas flowing in the minichannel. The effect of the e-folding time on the transient heat transfer was investigated. However, correlations of steady-state and transient heat transfer have not been reported.

Recent reviews on microchannels and minichannels [5, 19] show disagreement between researchers on whether the classical theory of conventional channel is suitable for microchannel and minichannel. Further, the influence of minichannels on the performance of forced convective heat transfer for helium gas in the turbulent flow region with a circular channel shape is not well established, and research on the gas and wall temperature effect is insufficient. In this study, the heat transfer process of the turbulent flow of helium gas through a minichannel was analyzed. A circular minichannel fabricated by platinum with an inner diameter of 1.8 mm was employed as the test heater. An exponentially increasing heat input was supplied to the test tube. The heat flux and the surface temperature were measured for different experimental conditions such as e-folding time of the heat generation rate, inlet gas temperatures, and flow velocities. The obtained heat transfer performance was compared to the classical correlations of the conventional channel. Further, a new semi-empirical correlation was derived using substantial experimental data.

2. Experimental facility and method

2.1 Helium gas loop

The experimental facilities contained three main components: a helium gas loop, a heat input control system, and a data acquisition and analysis system. A schematic drawing of the helium gas loop reported by Liu et al. [20, 21] is illustrated in **Fig. 1**. The working fluid was pure helium gas provided by the pressurized gas cylinder. The test section had a horizontal layout in the gas loop. A vacuum pump was applied for the air discharge to maintain the purity of the working fluid during the experiment. The compressor was employed for the circulation of helium gas. The two surge tanks were used for gas storage and to eliminate any undulation associated with the gas flow. The

flow rate was measured using a turbine flow meter with a flow range of 11.3-85 L/min located before the test section. The lubricating oil leaked from the compressor and other particles were blocked by the filters to prevent them from damaging the flow meter and blocking the test section. The by-pass loops of the test section and the compressor were used to adjust the flow rate. The electrical pre-heaters and water-cooled cooler were utilized to control the gas temperature. The experimental devices mentioned above were connected with Swagelok parts and stainless-steel ducts, which can bear high pressure and prevent gas leakage. Additionally, the gas pressure and temperature at the flow meter outlet were measured by a pressure transducer and a K-type thermocouple, respectively.

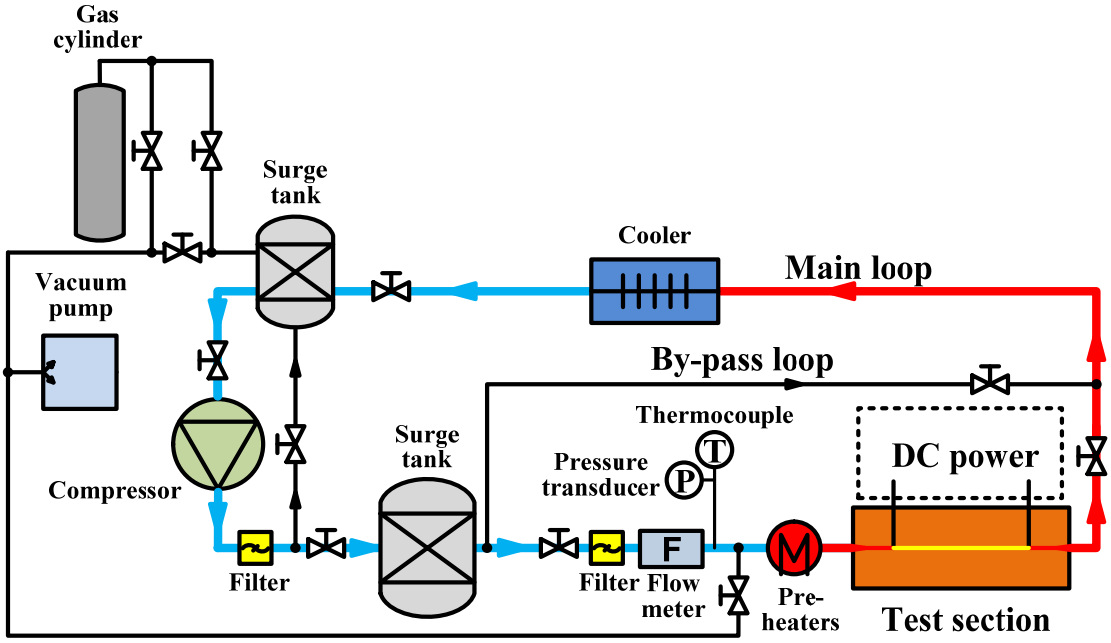

Fig. 1. Schematic drawing of helium gas loop.

2.2 Test section

Fig. 2 illustrates the details of the test section. A circular tube made of platinum with a commercially finished inner surface condition was installed horizontally in the test section. Its inner diameter, wall thickness, and total length were 1.8, 0.1, and 100 mm, respectively. Five millimeters of both the endpoints of the tube were inserted into the copper plates and connected via soldering. The copper plates were employed as electrodes for the current introduction. Therefore, the heated part, namely the effective length of the test tube (L_e), was 90 mm. The bakelites provided thermal insulation for the test tube from the surrounding environment and electric insulation for the test tube

from other metals in the test section. Two K-type thermocouples were installed in the center axis of the stainless-steel (SUS304) ducts before and after the test tube to measure the gas temperature. Two pressure transducers were utilized to measure the pressures at the entrance and exit of the test section. Further, the length of the entrance region with the same inner diameter as the test tube was 120 mm, which was sufficient to guarantee that the flow in the test tube was in the hydrodynamically fully developed region.

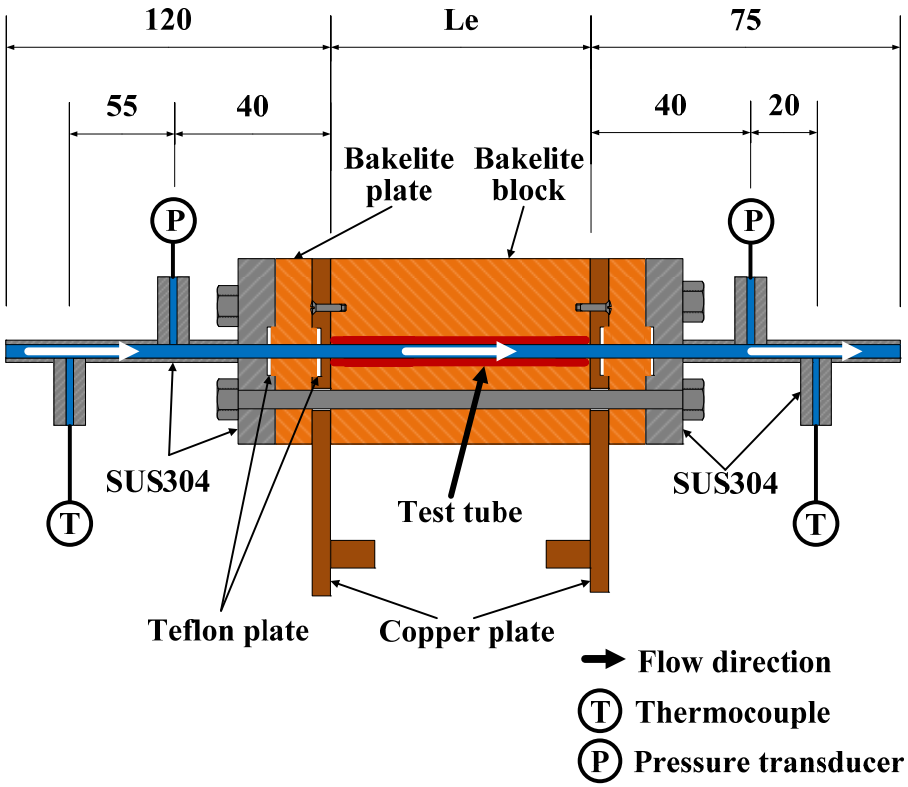

Fig. 2. Horizontal cross-sectional view of the test section.

2.3 Experimental procedure

As a preparation, the platinum tube was annealed to eliminate thermal stress. Further, it was washed with acetone liquid to remove impurities on the inner surface of tube. The relationship between the electrical resistance and temperature of the test tube was established by calibration in a deionized water bath. According to the calibration result, the relationship between resistance and the average temperature was expressed by the following equation:

$$R_T = 1.357 \times 10^{-2}(1 + 4.08 \times 10^{-3}T_a - 5.88 \times 10^{-7}T_a^2) \quad (1)$$

where R_T and T_a represent the measured resistance and average temperature of the test

tube, respectively.

The procedure of the main experiment is described as follows:

The test loop was sufficiently vacuumed, and then helium gas was filled in the test loop to attain designated pressure with all valves of the loop in the opening condition. This static condition was maintained to test the gas leakage. It was confirmed that there is no gas leakage before each experimental run. By starting the compressor, helium gas was circulated in the directions illustrated in **Fig. 1**. Before gas entered the test tube, the inlet gas was heated to desired temperatures with pre-heaters. After passing through the test tube, the hot gas was cooled down by the cooler and returned to the compressor to complete the circulation. The flow rate was raised from its minimum in a sequence by employing by-pass valves of the test section and the compressor. When the pressure, flow rate, and inlet gas temperature remained stable, a direct electrical current provided by a variable low-voltage power source was introduced to heat the test heater. The input heat was raised exponentially by using the heat input control system. The exponentially increasing heat generation rate of the test heater ($\dot{Q}$), is described as follows:

$$\dot{Q} = Q_0 \exp(t/\tau) \tag{2}$$

where Q_0, t, and τ are the initial heat generation rate, time, and e-folding time of the heat generation rate (the time needed for the heat generation rate to increase e times), respectively. When the average temperature reached the preset value, the power supply was cut off to protect the test heater. The experimental conditions are listed in **Table 1**. The data were collected and calculated by the data acquisition and analysis system during the entire experimental process.

Table 1 Experimental conditions.

Tube material	Platinum
Working fluid	Helium gas
Inner diameter	1.8 mm
Thickness	0.1 mm
Effective length	90 mm
e-folding time	1.5-15.3 s
Flow velocity	87-256 m/s
Inlet pressure	482-503 kPa
Inlet gas temperature	287-313 K
Reynolds number	5000-16000

2.4 Measurement method

The measurement method was like that in the experiment carried out by Shibahara et al. [22]. The test tube was employed as one branch of the double-bridge circuit, as shown in **Fig. 3**. By resistance thermometry, the average temperature of the test tube could be obtained from the variable resistance. Before electrical heating, the temperature was maintained at a constant level, and the electric equilibrium was acquired by adjusting the resistances of the double-bridge circuit. The electric nonequilibrium occurred with a change in the resistance induced by the heat input. With the measurement of the unbalanced voltage (V_T), the resistance of the test tube (R_T) is expressed as:

$$R_T = \frac{V_T(R_2+R_3)}{IR_2} + \frac{R_1R_3}{R_2} \tag{3}$$

The heat generation rate (Q) due to Joule heating is described as follows:

$$Q = V_R \frac{V_I}{R_s} \tag{4}$$

where V_R and V_I are the voltage drops across the test heater and the standard resistor (R_s), respectively. The V_T, V_R, and V_I signals were amplified by amplifiers and simultaneously sampled using an analog-to-digital converter.

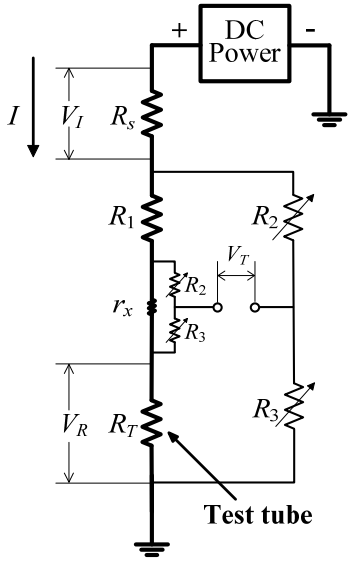

Fig. 3. Diagrammatic drawing of the double-bridge circuit.

The heat flux (q) on the inner surface of the heated tube is calculated from the heat input excluding the energy storage due to the increased average temperature of the test tube. The expression is as follows:

$$q(t) = \frac{V}{A}\left(\dot{Q}(t) - \rho_h c_h \frac{dT_a}{dt}\right) \tag{5}$$

where V, A, ρ_h, and c_h represent the volume, inner surface area, density, and specific heat of the test heater, respectively. The average temperature of the test heater was obtained by **Eq. (1)**. It should be mentioned that the heat loss from the outer surface of the test tube is negligible because the test tube is installed in a small closed space.

It can be assumed that the heat transfer process is under the quasi-steady condition with a relatively long e-folding time (see Section 3.3). An increase in the heat generation rate is relatively slow due to the passage of long elapsed time under a quasi-steady state. The inner surface temperature (T_s) can be calculated by solving a one-dimensional steady-state heat conduction differential formula, with the surface temperature around the heated tube being assumed as uniform. The expression is as follows:

$$\frac{d^2T}{dr^2} + \frac{1}{r}\frac{dT}{dr} + \frac{\dot{Q}}{\lambda} = 0 \tag{6}$$

Boundary conditions are expressed by the following equations:

$$q = -\lambda \frac{dT}{dr}\Big|_{r=r_i} \tag{7}$$

$$\frac{dT}{dr}\Big|_{r=r_o} = 0 \tag{8}$$

The temperature distribution ($T(r)$) and the average temperature (T_a) of the test heater are expressed as:

$$T(r) = -\frac{\dot{Q}r^2}{4\lambda} + \frac{\dot{Q}r_o^2}{2\lambda}\ln r + C \tag{9}$$

$$T_a = \frac{1}{\pi(r_o^2 - r_i^2)}\int_{r_i}^{r_o} 2\pi r T(r) dr \tag{10}$$

Then, the inner surface temperature (T_s) and the outer surface temperature (T_{so}) are given by:

$$T_s = T(r_i) = T_a - \frac{qr_i}{4(r_o^2 - r_i^2)^2\lambda} \times \left[4r_o^2\left\{r_o^2\left(\ln r_o - \frac{1}{2}\right) - r_i^2\left(\ln r_i - \frac{1}{2}\right)\right\} - (r_o^4 - r_i^4)\right] - \frac{qr_i}{2(r_o^2 - r_i^2)\lambda}(r_i^2 - 2r_o^2\ln r_i) \tag{11}$$

$$T_{so} = T(r_o) = T_a - \frac{qr_i}{4(r_o^2 - r_i^2)^2\lambda} \times \left[4r_o^2\left\{r_o^2\left(\ln r_o - \frac{1}{2}\right) - r_i^2\left(\ln r_i - \frac{1}{2}\right)\right\} - (r_o^4 - r_i^4)\right] - \frac{qr_ir_o^2}{2(r_o^2 - r_i^2)\lambda}(1 - 2\ln r_o) \tag{12}$$

$$C = T_a - \frac{qr_i}{4(r_o^2 - r_i^2)^2\lambda} \times \left[4r_o^2\left\{r_o^2\left(\ln r_o - \frac{1}{2}\right) - r_i^2\left(\ln r_i - \frac{1}{2}\right)\right\} - (r_o^4 - r_i^4)\right] \tag{13}$$

The entrance and exit pressures of the test tube are acquired from the pressures measured by the pressure transducers, which are located 40 mm before and after the test tube. The expressions are as follows:

$$P_{in} = P_{ipt} - (P_{ipt} - P_{opt}) \times \frac{0.04}{0.08+L_e} \quad (14)$$

$$P_{out} = P_{in} - (P_{in} - P_{opt}) \times \frac{L_e}{0.04+L_e} \quad (15)$$

It was observed that the flow velocity was relatively high in the minichannel. Then, the Mach numbers at the inlet and outlet of the test tube were estimated for each experimental condition. The average Mach number between the inlet and outlet of the test tube was confirmed to be lower than 0.3 under all experimental conditions. Therefore, the compressibility effect of helium gas in this research can be neglected.

An energy balance expression is used to obtain the outlet gas temperature (T_{out}) as follows:

$$T_{out} = T_{in} + \frac{4L_e q}{uc_{p,g}\rho_g d} \quad (16)$$

The fluid physical properties are acquired by using the following gas bulk temperature (T_g) as the reference temperature. The expression is as follows:

$$T_g = (T_{in} + T_{out})/2 \quad (17)$$

The estimated maximum errors for the heat generation rate, heat flux, and inner surface temperature of the test tube were equal to ±2%, ±2.4%, and ±1 K, respectively [12].

3 Experimental results and discussion

3.1 Variation of heat generation rate, heat flux, and inner surface temperature with elapsed time

It is confirmed that the variation trend of the heat generation rate, inner surface temperature, and heat flux with elapsed time is identical under all experimental conditions. **Fig. 4** illustrates the representative experimental data for flow velocities of 143 and 208 m/s, e-folding time of 1.5, 7.5, and 14.9 s, and inlet gas temperature of 287 K. **Fig. 4 (i)** displays the exponential increase in the heat generation rate with elapsed time following **Eq. (2)**. Further, as shown in **Fig. 4 (ii)** and **(iii)**, the heat flux and tube inner surface temperature exponentially increase with the exponential increase in heat supply. The increase in the heat generation rate, inner surface temperature, and heat flux is quicker for shorter e-folding time. Furthermore, at the same e-folding time, the heat generation rate and heat flux become larger with the increase in the elapsed time as the flow velocity increases. However, the maximum inner surface temperature is approximately the same for different flow velocities and e-folding time. The inner

surface temperature under higher flow velocity requires a longer elapsed time to attain the preset protective temperature. Under the same e-folding time and elapsed time, the heat flux and heat generation rate under the flow velocity of 208 m/s are almost the same as those of 143 m/s, but the inner surface temperature is lower under higher flow velocity. It means that the quantity of heat applied to the test tube is removed more by higher flow velocity so that the test tube can withstand more heat load. The effect of flow velocity on thermal characteristics is discussed in detail in Section 3.3.

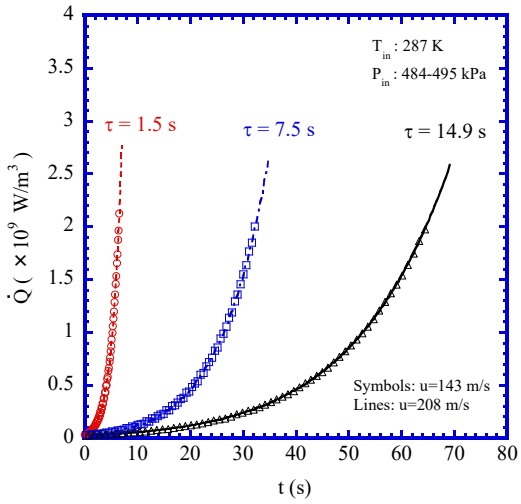

(i) Heat generation rate $\dot{Q}$

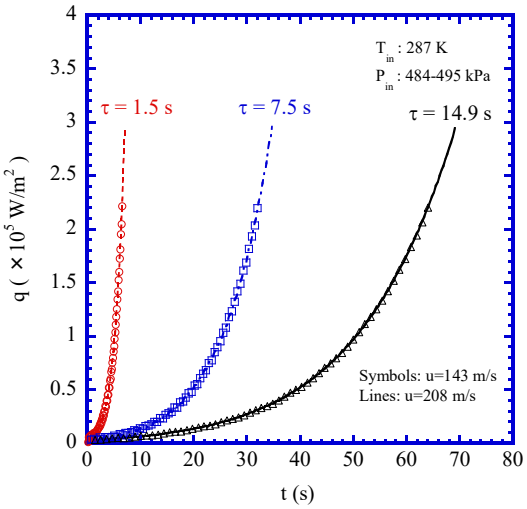

(ii) Heat flux q

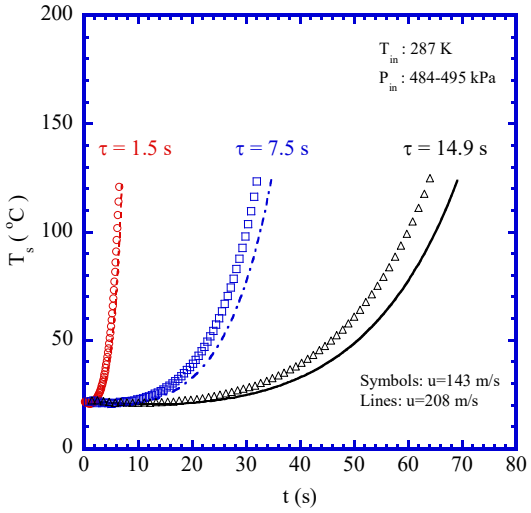

(iii) Inner surface temperature T_s

Fig. 4. Variation of heat generation rate, heat flux, and inner surface temperature with time.

3.2 Comparison with classical correlations

The temperature difference between the inner surface temperature and gas bulk temperature (ΔT), and the heat transfer coefficient (h) are given by:

$$\Delta T = T_s - T_g \quad (18)$$

$$h = q/\Delta T \quad (19)$$

The Nusselt number (Nu_f), Reynolds number (Re_f), and Prandtl number (Pr_f) used in this research are defined by the following equations:

$$Nu_f = hd/\lambda;\ Re_f = ud/\nu;\ Pr = \nu/a \quad (20)$$

To compare the experimental data on the heat flux as a function of temperature difference with values predicted by classical correlations, three well-known correlations applied to conventional channels are introduced.

In the case of the heat transfer process for forced convection in conventional channels, the longest and most universal correlation was proposed by Dittus and Boelter [23] as follows ($Re > 10^4$):

$$Nu_f = 0.023 Re_f^{0.8} Pr_f^{0.4} \quad (21)$$

Another well-known expression for fluid flowing through conventional channels in a fully developed turbulent region with higher accuracy was suggested by Petukhov [24] as follows ($10^4 < Re < 5 \times 10^6$):

$$Nu_f = \frac{(f/8) Re_f Pr_f}{1.07 + 12.7 (f/8)^{1/2} (Pr_f{}^{2/3} - 1)} \quad (22)$$

where

$$f = (1.82log_{10}Re_f - 1.64)^{-2} \quad (23)$$

Moreover, it is desirable to present a comparison in the laminar-turbulent transition region. The modification of Petukhov correlation suggested by Gnielinski [10] is expressed as ($2300 < Re < 5 \times 10^6$):

$$Nu_f = \frac{(f/8)(Re_f - 1000)Pr_f}{1+12.7(f/8)^{1/2}(Pr_f{}^{2/3}-1)} \quad (24)$$

Fig. 5 illustrates the comparison between the typical experimental data and prediction values. A linearly increasing heat flux can be found with an increase in the temperature difference on log-log graphs. It is understood that the heat transfer process becomes stable at higher temperature differences. As shown in **Fig. 5 (i)**, the heat flux obtained from experimental data is 42% higher than the value calculated by Gnielinski correlation at a temperature difference of 40 K in the laminar-turbulent transition region ($2300 < Re < 10^4$). As indicated in **Fig. 5 (ii)**, the experimentally obtained data are always higher than the predicted values of the three classical correlations at the same temperature difference in the fully developed turbulent region ($Re > 10^4$). The results reveal the heat transfer augmentation in the turbulent flow of helium gas through a minichannel compared with a traditional channel. It is supposed that a thinner thermal boundary layer near the inner surface of the minichannel leads to the above experimental phenomena [12]. Therefore, the classical correlations aiming at conventional channels are not appropriate for predicting the heat transfer performance on the turbulent flow of helium gas inside the minichannel.

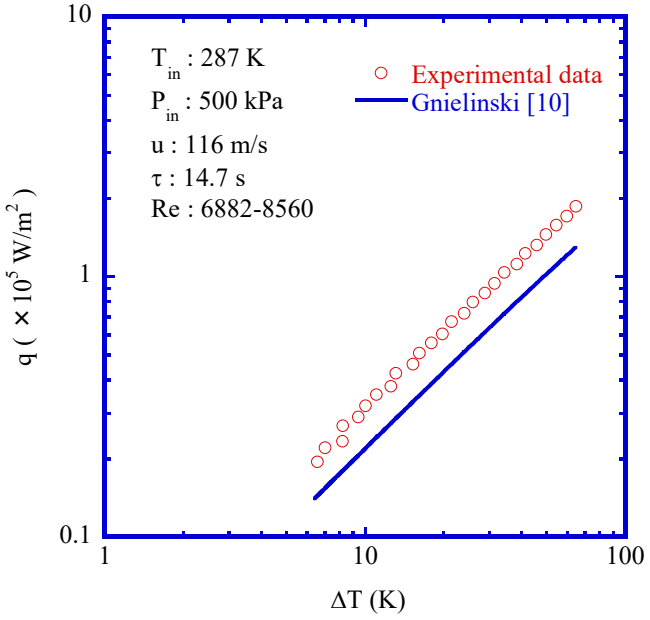

(i) $Re < 10000$

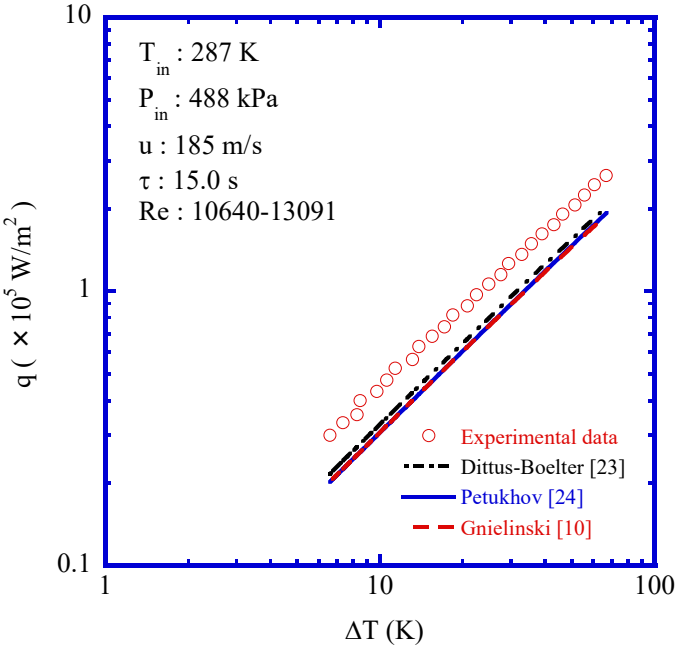

(ii) $Re > 10000$

Fig. 5. Experimental data for the relation of the heat flux with the temperature difference compared to predicted values of classical correlations.

3.3 Effect of e-folding time, flow velocities, and inlet gas temperatures on heat transfer coefficients

Fig. 6 shows the heat transfer coefficients as a function of the e-folding time ranging from 1.5 to 14.9 s, at temperature differences ranging from 30 to 60 K, under a flow velocity of 171 m/s. There is no obvious deviation in the heat transfer coefficients between different temperature differences at the same e-folding time, as illustrated in **Fig. 6**. It can be confirmed that heat transfer coefficients at temperature differences of 30, 40, 50, and 60 K are achieved from the stable part illustrated in **Fig. 5**. The data obtained from the experiment at temperature differences of 30, 40, 50, and 60 K are analyzed for different experimental conditions. Moreover, there is no significant effect of the e-folding time on the heat transfer coefficients for each temperature difference because the e-folding time ranges from 1.5 to 14.9 s, which is relatively long. The thermal boundary layer adjacent to the inner surface of the test tube has enough time for fully development. The heat transfer in this range of the e-folding time can be classified as quasi-steady-state heat transfer.

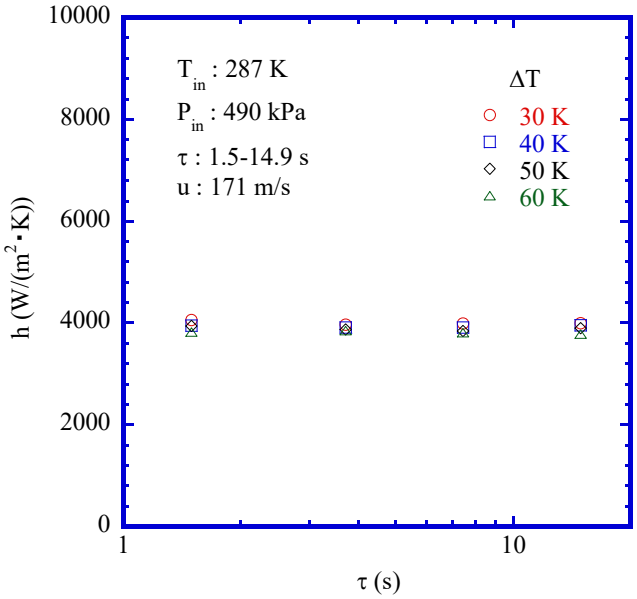

Fig. 6. Heat transfer coefficients as a function of e-folding time under various temperature differences.

Fig.7 indicates the heat transfer coefficients as a function of e-folding time in the range of 1.5 to 15.2 s, and for flow velocities ranging from 87 to 241 m/s, at the temperature difference of 50 K. Identical heat transfer coefficients with e-folding time varied from 1.5 to 15.2 s are found at each flow velocity. It is confirmed that the heat transfer process at each flow velocity is under quasi-steady-state conditions. The heat transfer coefficients increase when flow velocities increase for the same e-folding time, which indicates the domination of convective heat transfer in the quasi-steady-state heat transfer process.

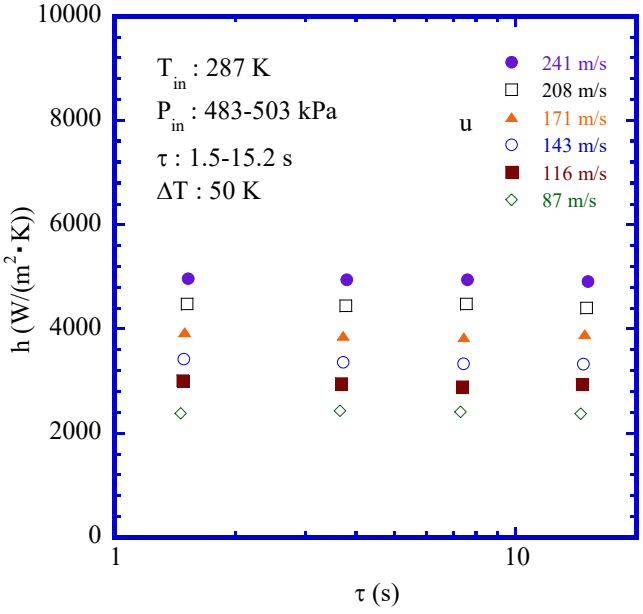

Fig. 7. Heat transfer coefficients as a function of e-folding time under different flow

velocities.

Fig. 8 illustrates the relation of the heat transfer coefficients with inlet gas temperatures in the range of 287 to 313 K, and for flow velocities ranging from 193 to 256 m/s, at a temperature difference of 40 K. The heat transfer coefficients exhibit a weak dependence on inlet temperatures of helium gas for all flow velocities. This experimental phenomenon is also found at each e-folding time.

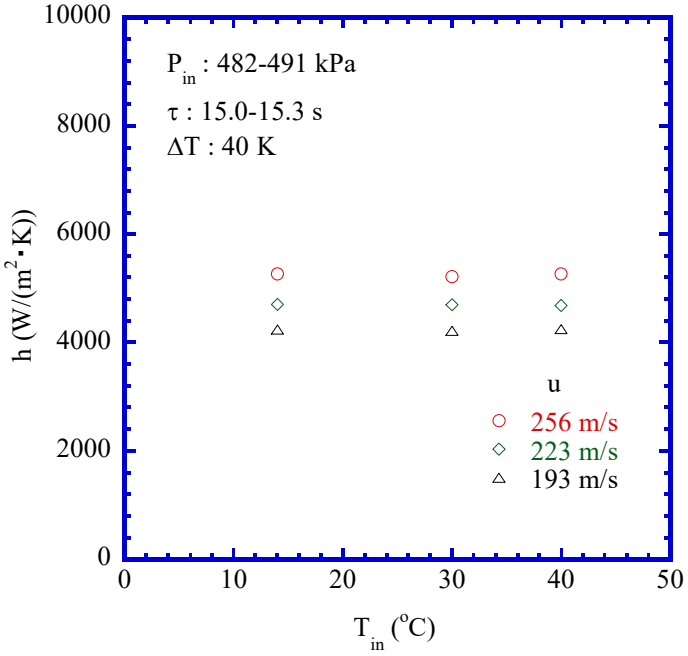

Fig. 8. Heat transfer coefficients as a function of inlet gas temperatures under different flow velocities.

3.4 An empirical correlation for turbulent heat transfer in minichannel

Re primarily depends on flow velocity and *Nu* is mainly affected by the heat transfer coefficient at the constant fluid property and channel size. The dependence of *Nu* on *Re* can be inferred by the relationship between the heat transfer coefficient and flow velocity. **Fig. 9** illustrates the relation of the heat transfer coefficients with flow velocities at temperature differences of 30, 40, 50, and 60 K on the log-log graph. The heat transfer coefficients show a linear increment with increasing flow velocities for each temperature difference. The slope (n), estimated by the method of least-squares, is 0.8 on the log-log coordinate figure.

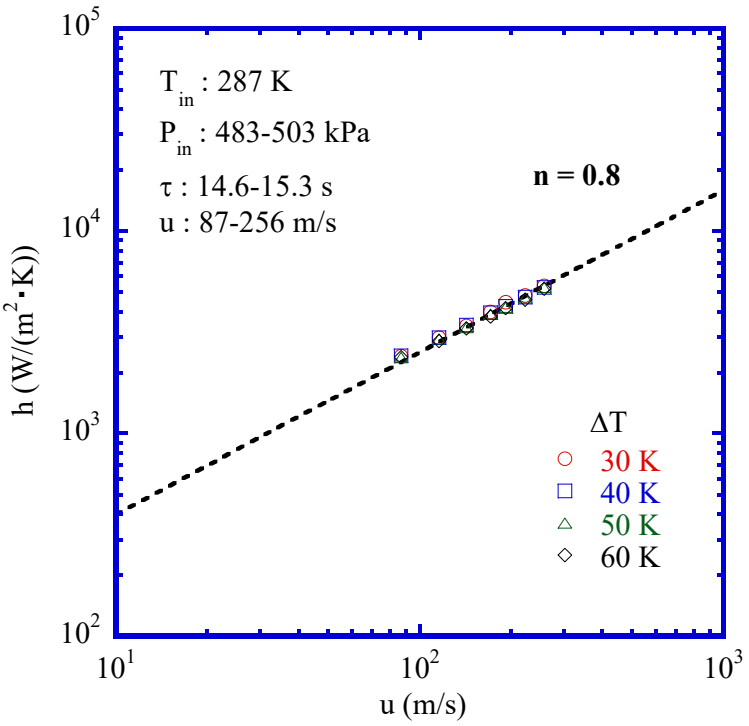

Fig. 9. The slope of heat transfer coefficients versus flow velocities.

The dependence of physical properties on the gas temperature affects the convective heat transfer process. Concerning forced convection for gas in the channel, Petukhov [24] suggested using the ratio of surface temperature to gas bulk temperature to research the influence of physical properties on the gas heat transfer process. **Fig. 10** displays the effect of the inner surface temperature versus the gas bulk temperature on the heat transfer coefficients for flow velocities in the range of 116 to 208 m/s. For each flow velocity, the heat transfer coefficients show a linear decline with n = -0.5, as the ratio of the inner surface temperature to the gas bulk temperature increases on the log-log graph. Under tube heating conditions, the dynamic viscosity near the inner surface is always higher than that in the mainstream, because the dynamic viscosity increases as the gas temperature increases. The heat transfer is weakened due to the reduction in the velocity gradient adjacent to the surface caused by higher viscosity. The viscosity difference between the near wall and mainstream increases gradually as the ratio of surface temperature to gas bulk temperature increases, which leads to decreasing heat transfer coefficients. The parameter of $(T_s/T_g)^{-0.5}$ is the same as that applied in many correlations reported by Petukhov [24].

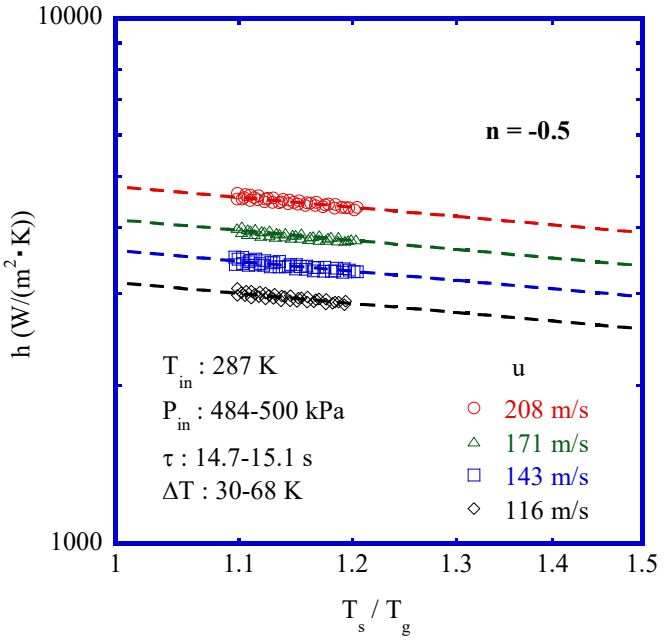

Fig. 10. The slope of heat transfer coefficients versus T_s/T_g.

According to the classical Dittus-Boelter expression [23], during fluid heating, the exponent of Pr is 0.4. Thus, $Pr^{0.4}$ is employed as a parameter in our correlation. The experimental data under quasi-steady conditions are plotted in **Fig. 11** for inlet gas temperatures of 287, 303, and 313 K, inlet pressures ranging from 482 to 503 kPa, temperature differences of 30, 40, 50, and 60 K, and flow velocities ranging from 87 to 256 m/s. A semi-empirical correlation for helium gas flowing in the circular tube with an inner diameter of 1.8 mm is obtained based on the experimental data as follows:

$$Nu_f = 0.0333 Re_f^{0.8} Pr_f^{0.4} (T_s/T_g)^{-0.5} \quad (25)$$

As shown in **Fig. 11**, the solid line represents **Eq. (25)**. Notably, a substantial amount of experimental data fall within a ±10% deviation of **Eq. (25)**, which means that the correlation has a relatively high accuracy. The new correlation includes the laminar-to-turbulent transition region and the fully developed turbulent region.

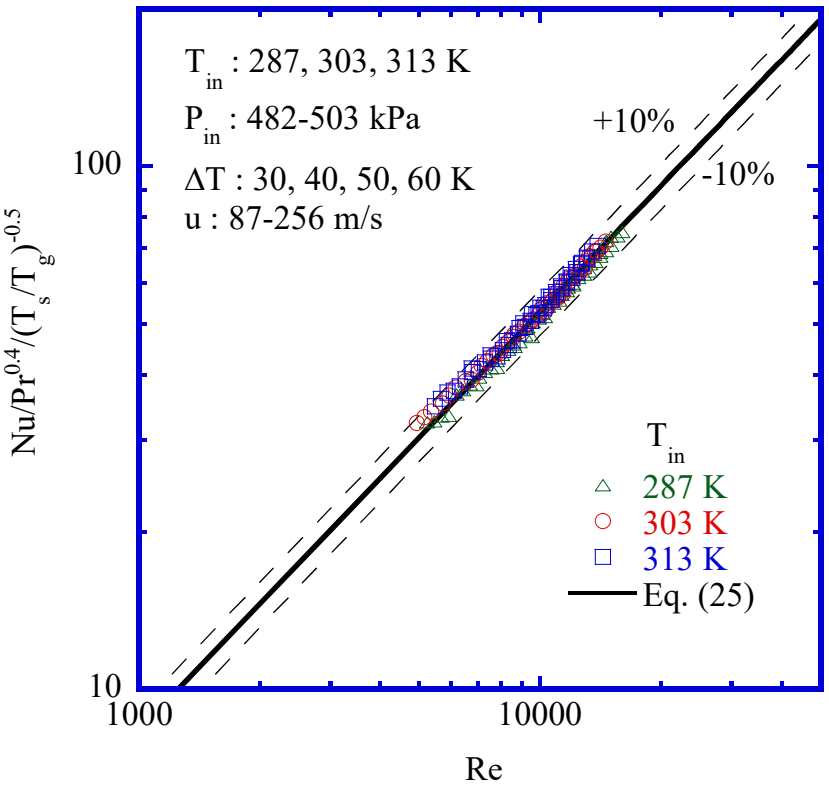

Fig. 11. Empirical correlation for helium gas flowing in minichannel.

3.5 Comparison with previous heat transfer correlation for water in a minichannel

The correlations suggested by Shibahara et al. [25] for water flowing in circular tubes with inner diameters of 1 and 2 mm are described as follows:

$Nu_f = 0.023Re_f^{0.85}Pr_f^{0.4}(L_e/d)^{-0.08}(\mu/\mu_w)^{-0.14}$ (d: 2.0 mm; deviation: ±20%) (26)

$Nu_f = 0.001Re_f^{1.2}Pr_f^{0.4}(L_e/d)^{-0.08}(\mu/\mu_w)^{-0.14}$ (d: 1.0 mm; deviation: ±30%) (27)

where μ and μ_w are obtained using fluid bulk temperature and tube surface temperature as a reference, respectively. There are no available experimental data of **Eq. (27)** in the laminar-to-turbulent transition region. All the experimental data are calculated by introducing parameters of $(L_e/d)^{-0.08}$ and $(\mu/\mu_w)^{-0.14}$ to compare with **Eq. (26)** and **Eq. (27)**. **Fig. 12** shows that our experimental data are higher than the values obtained using **Eq. (26)** and lower than the values obtained using **Eq. (27)**. Most of the data are 20% higher than the correlation with the 2-mm channel. The tube used in this research is 1.8 mm, which is a little smaller than the inner diameter used in **Eq. (26)**. According to the result suggested by Shibahara et al. [25], a higher heat transfer coefficient can be obtained by using a smaller diameter tube. As a result, it is reasonable that our

experimental data (5000 < *Re* < 16000) are higher than those obtained from **Eq. (26)**. The deviation of the novel correlation for turbulent heat transfer in minichannel is ±10%, which is more suitable for the turbulent flow of helium gas in minichannel. In future research, the impact of minichannel size on the heat transfer process using helium gas will be analyzed.

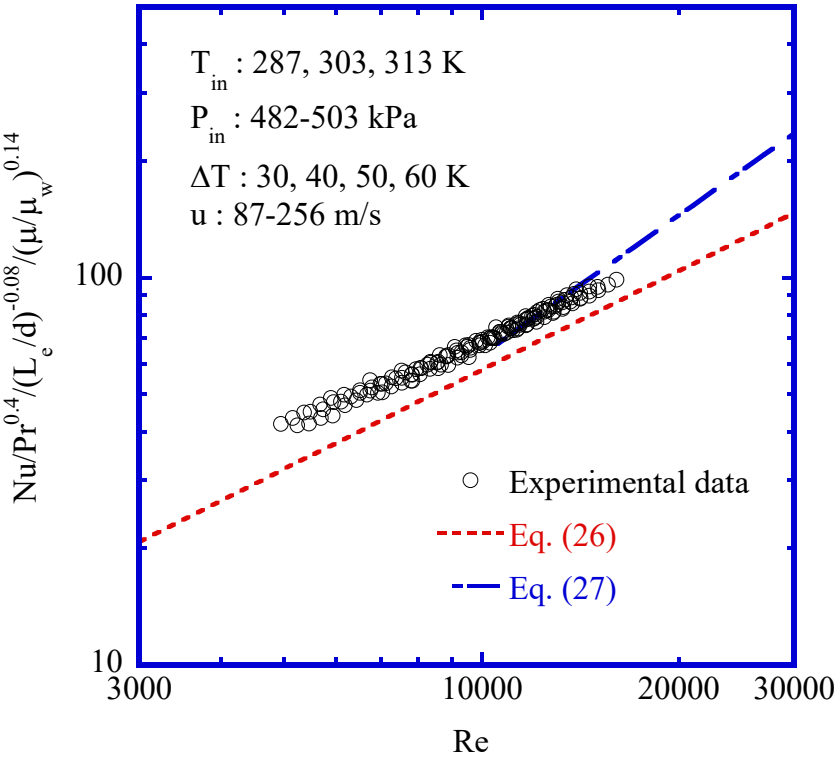

Fig. 12. Comparison with other correlation of minichannel.

4 Conclusions

A comprehensive experimental study was conducted on the heat transfer performance for turbulent flow of helium gas through a minichannel by exponentially increasing heat generation rate under extensive experimental conditions, such as different e-folding time of the heat generation rate, inlet gas temperatures, and flow velocities. The conclusions are as follows:

(1) The heat transfer process on forced convection of helium gas through the minichannel was enhanced compared with classical correlations applicable to conventional large size channels in the turbulent region.

(2) The increase in flow velocity increased the heat transfer coefficients, but the heat transfer coefficients showed a decreasing trend with an increase in T_s/T_g. Moreover, the influence of the e-folding time and inlet gas temperature on the heat transfer

coefficient was not significant under quasi-steady conditions ($\tau > 1.5$ s).

(3) A new semi-empirical correlation for turbulent flow of helium gas in a minichannel with a difference of ±10% was obtained using the non-dimensional parameters: *Nu*, *Re*, *Pr*, and T_s/T_g.

Acknowledgement

This research was funded by the Japan Society for the Promotion of Science (JSPS) (Grant-in Aid for Scientific Research (C), KAKENHI, No. 18K03979).

References

[1] M. S. Tillack, P. W. Humrickhouse, S. Malang, R. E. Nygren, Technology readiness of helium as a fusion power core coolant, UCSD-CER-14-03, Center for Energy Research, University of California, San Diego, December 2014.

[2] L.V. Boccaccini, L. Giancarli, G. Janeschitz, S. Hermsmeyer, Y. Poitevin, A. Cardella, E. Diegele, Materials and design of the European DEMO blankets, Journal of Nuclear Materials 329-333 (2004) 148-155.

[3] B. Xiang, X. F. Ye, K. M. Feng, Conceptual and preliminary engineering design of experimental helium loop for China HCCB TBM components test, Fusion Engineering and Design 85 (2010) 2146-2149.

[4] F. Dobran, Fusion energy conversion in magnetically confined plasma reactors, Progress in Nuclear Energy 60 (2012) 89-116.

[5] T. Dixit, I. Ghosh, Review of micro- and mini-channel heat sinks and heat exchangers for single phase fluids, Renewable and Sustainable Energy Reviews 41 (2015) 1298-1311.

[6] S. G. Kandlikar, Fundamental issues related to flow boiling in minichannels and microchannels, Experimental Thermal and Fluid Science 26 (2002) 389-407.

[7] Y. Nakamura, Q. S. Liu, M. Shibahara, K. Hata and K. Fukuda, Transient turbulent heat transfer in vertical small tube, Journal of the JIME 53 (6) (2018) 137-144.

[8] N. T. Nguyen, D. Bochnia, R. Kiehnscherf, W. Dötzel, Investigation of forced convection in microfluid systems, Sensors and Actuators A 55 (1996) 49-55.

[9] T. M. Adams, S. I. Abdel-Khalik, S. M. Jeter, Z. H. Qureshi, An experimental investigation of single-phase forced convection in microchannels, International Journal of Heat and Mass Transfer 41 (6-7) (1998) 851-857.

[10] V. Gnielinski, New equations for heat transfer in turbulent pipe and channel flow, International Chemical Engineering 16 (2) (1976) 359-368.

[11] B. M. Dai, M. X. Li, C. B. Dang, Y. T. Ma, Q. Chen, Investigation on convective heat transfer characteristics of single phase liquid flow in multi-port micro-channel tubes, International Journal of Heat and Mass Transfer 70 (2014) 114-118.

[12] Y. T. Li, K. Fukuda, Q. S. Liu, M. Shibahara, Turbulent heat transfer with FC-72 in small diameter tubes, International Journal of Heat and Mass Transfer 103 (2016) 428-434.

[13] Y. T. Li, K. Fukuda, Q. S. Liu, Transient heat transfer due to exponentially increasing heat inputs for turbulent flow of FC-72 in small diameter tubes, International Journal of Heat and Mass Transfer 110 (2017) 880-889.

[14] W. Owhaib, B. Palm, Experimental investigation of single-phase convective heat transfer in circular microchannels, Experimental Thermal and Fluid Science 28 (2004) 105-110.

[15] S. K. Mylavarapu, X. D. Sun, R. E. Glosup, R. N. Christensen, M. W. Patterson, Thermal hydraulic performance testing of printed circuit heat exchangers in a high-temperature helium test facility, Applied Thermal Engineering 65 (2014) 605-614.

[16] A. J. Jiao, S. Jeong, H. B. Ma, Heat transfer characteristics of cryogenic helium gas through a miniature tube with a large temperature difference, Cryogenics 44 (2004) 859-866.

[17] F. Arbeiter, Experimental and numerical investigations on minichannel cooling gas thermal-hydraulics, in: Proceedings of the 15th International Conference on Nuclear Engineering, ICONE15-10514, Nagoya, 2007, pp. 1-8.

[18] F. Xu, Q. S. Liu, S. Kawaguchi, M. Shibahara, Experimental study on transient heat transfer for helium gas flowing in a minichannel, in: Proceedings of the 2020 International Conference on Nuclear Engineering, ICONE2020-16697, Virtual, Online, 2020, pp. 1-6.

[19] J. Z. Zhou, X. L. Cao, N. Zhang, Y. P. Yuan, X. D. Zhao, D. Hardy, Micro-channel heat sink: a review, Journal of Thermal Science 29 (6) (2020) 1431-1462.

[20] Q. S. Liu, M. Shibahara, K. Fukuda, Transient heat transfer for forced convection flow of helium gas over a horizontal plate, Experimental Heat Transfer 21 (2008) 206-219.

[21] Q. S. Liu, Z. Zhao, K. Fukuda, Experimental study on transient heat transfer

enhancement from a twisted plate in convection flow of helium gas, International Journal of Heat and Mass Transfer 90 (2015) 1160-1169.

[22] M. Shibahara, K. Fukuda, Q. S. Liu, K. Hata, Steady and transient critical heat flux for subcooled water in a mini channel, International Journal of Heat and Mass Transfer 104 (2017) 267-275.

[23] F. W. Dittus, L. M. K. Boelter, Heat transfer in automobile radiators of tubular type, University of California Press, Berkeley, University of California Publications in Engineering 2 (13) (1930) 443–461.

[24] B. S. Petukhov, Heat transfer and friction in turbulent pipe flow with variable physical properties, Advances in Heat Transfer 6 (1970) 503-564.

[25] M. Shibahara, K. Fukuda, Q. S. Liu, K. Hata, Steady and transient forced convection heat transfer for water flowing in small tubes with exponentially increasing heat inputs, Heat Mass Transfer 53 (2017) 787-797.